

Composite square and monomial power sweeps for SNR customization in acoustic measurements

Csaba Huszty (1), Shinichi Sakamoto (2)

(1) Graduate School, The University of Tokyo
 (2) Institute of Industrial Science, The University of Tokyo

PACS: 43.20.Ye 43.58.Gn 43.55.Mc

ABSTRACT

Swept signals for acoustic measurements are widely used nowadays to obtain impulse responses of the system under test. The overall spectrum and the inverse filter that compresses the sweep into an impulse together with the background noise conditions prescribe the result's signal-noise-ratio as a function of frequency. This paper proposes a time-domain sweep synthesis method using composite square and monomial power frequency modulated sine sweeps that can customize the resulting SNR-frequency function. Theoretical and practical aspects as well as measurement results are presented.

INTRODUCTION

Impulse response or transfer function measurements play a key role in linear acoustics. Various measurement signals are used to obtain the measurement results, such as direct impulse-like excitations, random or pseudo-random signals such as the MLS [1], or swept sines [2]. The latter signals are used to spread the energy of the impulses in time to support higher signal-noise ratio (SNR) in the obtained results. Sine sweeps can be constructed in the frequency domain (such as the TSP signals, [3]) or in the time-domain. The sweep signals can be advantageously used if their overall spectrum can be customized. This was already proposed in the frequency domain [4,5], but in the time domain, analytic formulas were not present and applied yet widely except of two shapes, the linear sweep (having a white overall spectrum) and the exponential sweep (having a pink overall spectrum) [6].

In this paper we propose generating perfect-envelope sine sweeps in the time-domain with different sweep rates employing analytic formulae. Although this alone makes it possible to implement sweep signals with various overall spectra, in this paper we examine the possibility of using these signals expanded to square sweeps, and creating mixed composite square sweep signals sweeping at different frequency ranges at the same time. Lastly we examine measurement results obtained with these signals.

SINE, SQUARE AND COMPOSITE SWEEPS

Monomial sine sweep

In order to define controllable sweep rate signals with perfect envelope, in this present approach we propose to formulate sweeps in the time-domain, in the form

$$s(t) = A \cdot \sin(\Phi(t)) = A \cdot \sin\left(\int \omega(t) dt\right) \quad (1)$$

where A is the signal amplitude, ω is the angular frequency and $\Phi(t)$ is the momentary phase function. If we let v be a

general modulation function depending of t in the first order such that

$$\omega(t) = a \cdot v(b \cdot t + c) + d \quad (2)$$

where c and d are arbitrary constants and a and b are scaling functions prescribed by the frequency boundary conditions of the excitation signal, then by choosing $v = x^p$ we obtain the monomial higher order power sweep:

$$s(t)_{\text{mp}} = A \sin\left(\frac{T(\omega_1 - d)}{\eta c^p (p+1)} \left(\left(\frac{Tc + \eta t}{T}\right)^q - c^q\right) + d t\right) \quad (3)$$

where p is a free parameter and where

$$\eta = \frac{(c^p (\omega_2 - d))^{\frac{1}{p}}}{\omega_1 - d} - c \quad (4)$$

$$q = p + 1$$

to support shorter notation. Without further loss of generality let us assume that $(0 < \omega_1 < \omega_2 < \infty)$ so the signal starts at a non-zero frequency and excites a finite band.

The monomial sweep has considerable sweep rate customizability using the parameters c , d and p .

These parameters control different aspects of the signal, but in order to obtain real phase functions, c^p must be real. Consequently, if $c < 0$ then p must be an integer. Furthermore $c \neq 0$ and $p \neq 0$, and

$$d: \begin{cases} \omega_1 > d > \omega_2: & c^p > 0 \\ \omega_1 < d < \omega_2: & c^p < 0 \end{cases} \quad (5)$$

If d is chosen accordingly, then $|c|$ is redundant, only its sign matters together with the value of p .

Parameter d is controlling a spectrum bending feature: by setting a default $d=0$, perfectly pink, white, exponential or red (Brownian) overall spectrums can be obtained, but by changing d to a non-zero value, bended spectrums are obtained.

Despite that (3) is in a form where $p \neq -1$ must be met, it is true that the monomial power sweep generates a signal with an overall red (Brownian) spectrum, since:

$$\lim_{p \rightarrow -1} s(t)_{mp} = A \sin \left(\frac{(\omega_1 - d)T}{\ln \frac{\omega_2 - d}{\omega_1 - d}} \ln \left(\frac{t}{T} \frac{\omega_2 - d}{\omega_1 - d} - 1 \right) + 1 \right) + d t \quad (6)$$

When $c > 0$ and p tends to infinity the monomial sweep is equivalent to the generalized exponential sweep:

$$s(t)_{g.exp} = A \cdot \sin \left(\frac{(\omega_1 - d)T}{\ln \frac{\omega_2 - d}{\omega_1 - d}} \left[e^{\frac{t}{T} \ln \frac{\omega_2 - d}{\omega_1 - d}} - 1 \right] + dt \right) \quad (7)$$

Note that c is redundant in (7). This generalized exponential sweep can be used to synthesize various sweep shapes (Fig. 1).

The special case of complex

$$c^p = \frac{1}{\sqrt{-n}} \quad \text{where } n \in \mathbb{R}^+ \quad (8)$$

gives a single-frequency signal at angular frequency d . The region where c^p is positive (i.e. either c is positive or c is negative but p is even) can be effectively used to create sweeps that have different bended monotonic overall shapes between logarithmic-like, linear, exponential-like and more rapid than an exponential increase (Fig. 2).

Another useful feature of the monomial sweep is that it support frequency focus – making the signal spend more time at a particular angular frequency – within the band ω_1 and ω_2 can be achieved by setting

$$c < 0 \quad \text{and} \quad p = 2k + 1 \quad \text{where } k \in \mathbb{Z}^+ \quad (9)$$

and by increasing k the focus can be set to last longer relative to T (Fig. 3).

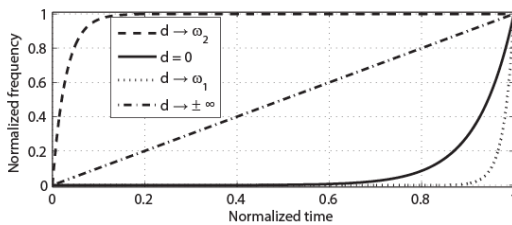


Figure 1. Different sweep rates of the generalized exponential sweep controlled by d . Curves of $d \rightarrow \omega_1$ and $d \rightarrow \omega_2$ are numeric examples using double precision.

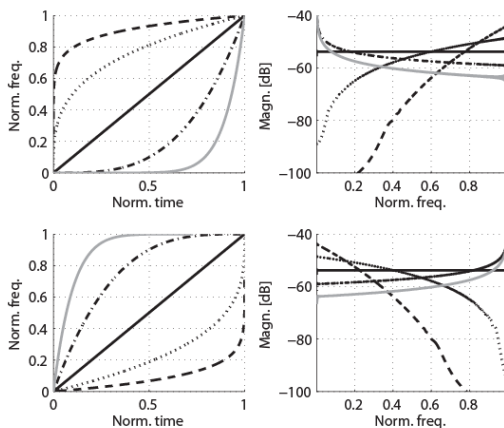


Figure 2. Monomial power sweep shapes in the $c^p > 0$ region; spectrogram (left) and spectrum (right). Solid line: $p = 1$, dotted line: $p = 0.3$, dashed line: $p = 0.1$, dashed dotted line: $p = 3.33$, Grey line: $p = 10$. Symmetry of $d = \omega_1 - \varepsilon$ (top) and $d = \omega_2 + \varepsilon$ (bottom) when $c > 0$.

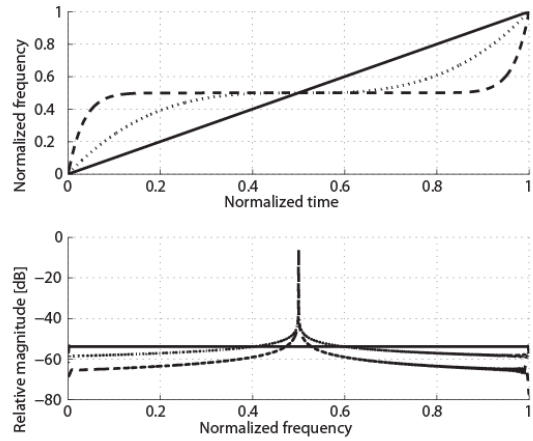


Figure 3. Frequency focus with monomial and sigmoid sweeps; spectrogram (left) and spectrum (right). Monomial power sweep with frequency focus on $d = 0.5 \cdot \omega_2$; dashed $p = 1$, dotted $p = 3$, solid $p = 7$, dotted dashed $p = 21$.

Composite square sweeps

Sine sweeps have many advantages when used in acoustic measurements; still, compared to MLS signals for example, they have a higher crest factor, meaning lower energy for the same peak amplitude. The crest factors are

$$C = \frac{\hat{x}}{x_{rms}}$$

$$C_{sine} = \frac{\max(|\sin(x)|)}{\lim_{T \rightarrow \infty} \frac{1}{\sqrt{2T}} \int_{-T}^T \sin^2(x) dx} = \sqrt{2} \quad (10)$$

$$C_{square} = \frac{\max(|\text{sgn}(\sin(x))|)}{\lim_{T \rightarrow \infty} \sqrt{\frac{1}{2T} \int_{-T}^T (\text{sgn}(\sin(x)))^2 dx}} = 1.$$

Sine sweeps can be transformed gradually into square-like signals by exploiting the Fourier-series expansion of the square signal. This way, as the series have more components, the crest factor of the signal will gradually decrease towards 0 dB. Since the number of components $M \in \mathbb{Z}^+$ is finite, the result is a sparsely distorted sweep:

$$s(t)_{SDS} = \frac{4 \cdot A}{\pi} \sum_{k=2l+1}^M \frac{1}{k} \cdot \sin(k \cdot \Phi(t)) \quad (11)$$

where $l \in \mathbb{Z}^+$, $\Phi(t)$ is the phase function. One advantage of a square sweep is that its fundamental harmonic, assuming $A = 1$ (full scale) is ‘encoded’ with a $\frac{4}{\pi}$ amplitude, which is almost 2.1 dBFS (higher than the full scale). It would be advantageous if this could be exploited somehow, however, the Gibbs ringing phenomenon, occurring at the discontinuities, and numeric limitations prevent the synthesis of signals without an overshoot. One way to mitigate this issue is to use smoothing, based on for example the Lanczos σ -approximation [7,8], which approximate a series according to:

$$s(\Phi)_L = \frac{a_0}{2} + \sum_{k=1}^{n-1} \sigma_n \cdot [a_k \cos(k\Phi) + b_k \sin(k\Phi)] \quad (12)$$

where $\sigma_n = \text{sinc}\left(\frac{k\pi}{n}\right)$ is the Lanczos σ -factor. This can be interpreted and generalized in this present ‘sparsely distorted sweep’ case to the formulation:

$$s(t)_{SDS,L} = \sum_{k=2l+1}^M \text{sinc}^\alpha \left(\frac{k\pi}{M+1} \right) \cdot \frac{1}{k} \cdot \sin(k \cdot \Phi(t)) \quad (13)$$

where α can be used to control the Gibbs ringing magnitudes; $\alpha \geq 1$ it effectively reduces overshooting; and by default $\alpha = 1$. Once the Lanczos-smoothing is used, the ‘encoded’ level of the first harmonic will be a function of the number of components, because σ is dependent of M (Fig. 4, middle). This prescribes a minimum number of components when the

signal can be effectively used (Fig. 4); in our present example of an exponential sweep, this yields the criterion $M > 8$. On the other hand, assuming $\alpha = 1$, $M > 12$ must be met in order to produce a higher energy signal than that is possible with the un-smoothed Fourier series.

This practically means that in an upwards exponential sweep ranging from 20 Hz to $f_s/2$ at a 48 kHz sampling frequency, we can use Lanczos-smoothed sparse distortion up to the time moment when the fundamental reaches $f_s/2/23$, so in this case, about 55% of the time can be artificially distorted in a way that it is ensured that the fundamental harmonic will be encoded with higher amplitude than the available full dynamic range.

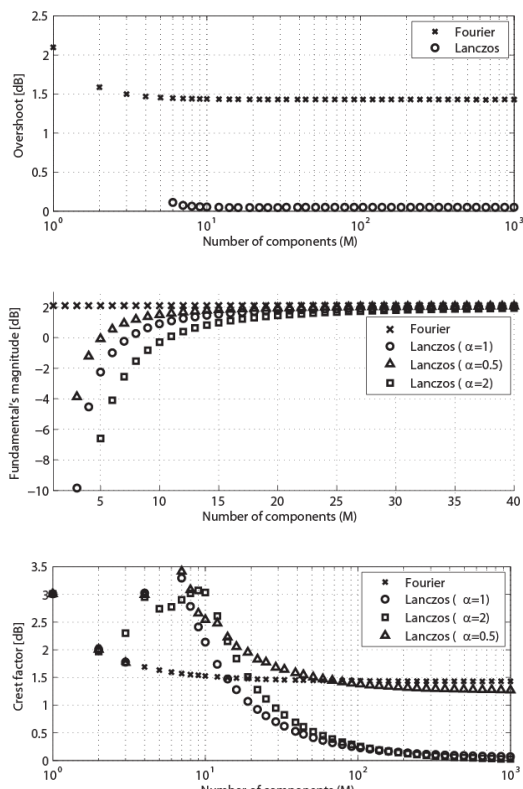


Figure 4. Overshoot of a 1-second, 0 dBFS targeted peak amplitude exponential square sweep generated by Fourier and Lanczos σ -approximated time series, $\alpha = 1$ (top); ‘encoded’ magnitude of the fundamental component (middle); overall crest factor (bottom). The lowest value on the horizontal axis is a perfect sine sweep; increasing values approximate the square sweep.

Without using the Lanczos-smoothing, a crest factor increase of about 1.5 dB seems to be maximally achievable, more or less independent of sweep frequency ranges, length and shape (except of extreme examples orthogonal to practice).

But more simply, a perfect square sweep can be obtained numerically by taking the sign function of the mother sine sweep:

$$s(t)_{\text{SQR}} = \lim_{k \rightarrow \infty} s(t)_{\text{SDS}} = A \cdot \text{sgn}\{\sin(\Phi(t))\} \quad (14)$$

Sparingly distorted sweeps and square sweeps both have similar frequency response magnitude shapes as their mother sine sweeps, but they use a wider (or full) available frequency range, feature more energy, up to 3 dB (shapes shown on Fig. 5) and their spectrum magnitudes are not as smooth as of a sine sweep’s.

Further band-based customization of the overall spectrum of the square and the sparsely distorted sweeps are possible by mixing various types of them. In general, mixing sweeps would most likely increase the crest factor of the result, and the lower energy for the same peak may not be practical, thus rather than mixing sine sweeps we propose to mix square sweeps instead. This also results in an increased crest factor, but we can still achieve higher energy content than what is possible with pure sine sweeps. Such composite sweeps can be synthesized by:

$$s(t)_C = \mathcal{N}\left\{\sum_{i=1}^N w_i \cdot s(t)_{\text{SQR},i}\right\} \quad (15)$$

where the \mathcal{N} operator denotes amplitude normalization, and w_i is an arbitrary gain factor.

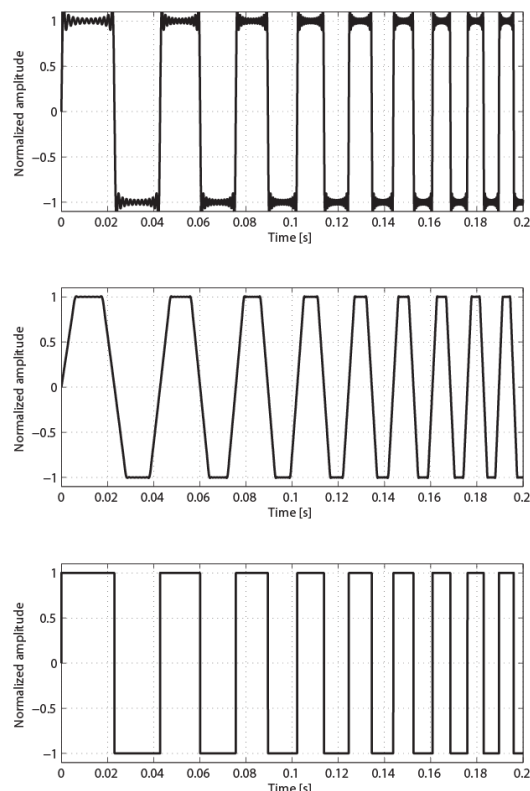


Figure 5. Time function of the beginning part of an 1-targeted amplitude exponential sweep, generated by a 12-term Fourier series (top), a 12-term Lanczos σ -approximated series with $\alpha = 1$ (middle) and by taking the sign of the mother sine sweep (bottom).

In practice, to allow frequency-response customization for example in octave bands, we mix two signals: the first signal $s(t)_{\text{SQR},1}$ sweeps in the full band, while the second signal $s(t)_{\text{SQR},2}$ sweeps in the octave band that is targeted for further noise suppression.

Since square sweeps have a non-smooth spectrum, when a composite square sweeps is formulated optimizing the overall spectrum into a particular frequency range, the obtainable spectrum is not smooth, therefore some fluctuations can be seen (Fig. 6). It is however easily possible to filter the wider-band square sweep and limit it to the first harmonic only in the range of the optimization sweep, this way little energy is lost but in the range of optimization smooth frequency result are obtainable (Fig. 7).

It is important to note that since the square sweep uses odd harmonics only, optimization in the interval of larger than

$$f_u \geq 3f_l \quad (16)$$

is advantageous, where f_u is the upper and f_l is the lower frequency limit of the desired band to optimize.

Inverse filters for each signals are constructed in the frequency domain by means of the H1 FRF estimator:

$$H_1(j\omega) = \frac{S_{SY}(j\omega)}{S_{SS}(j\omega)} \quad (17)$$

where $S_{SY}(j\omega)$ denotes the cross-spectrum of the noise-free input signal $S(j\omega)$ and the recorded signal $Y(j\omega)$.

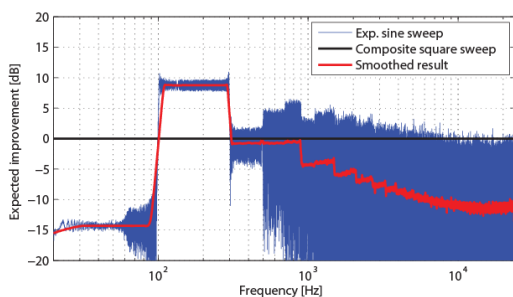


Figure 6. Expected SNR improvement by using a composite square sweep optimized for the 100-300 Hz band compared to a same-length exponential sine sweep. Overall crest factor is about 1.30 dB. Red shows smoothed blue.

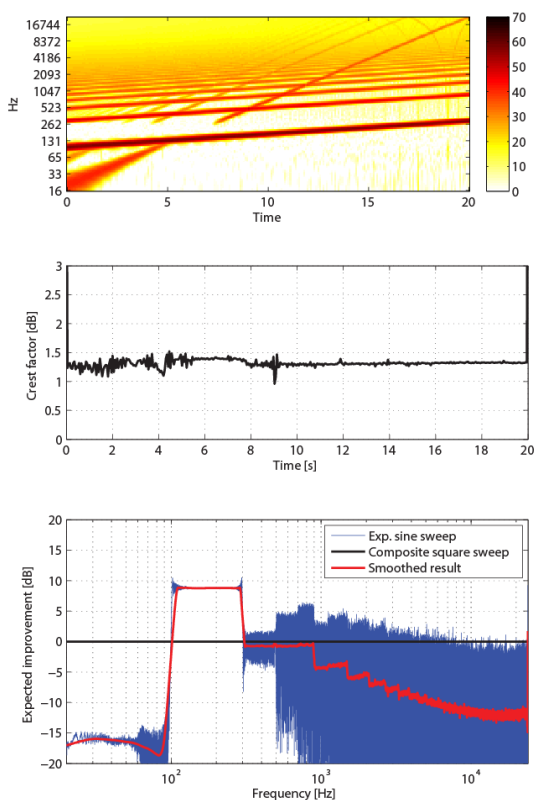


Figure 7. Spectrogram (top) of a filtered composite square sweep optimized for the band 100 to 300 Hz to support better noise suppression. Color scale is in dB. The short term (middle) as well as the overall crest factor is about 1.33 dB.

MEASUREMENT EXAMPLES

In this section a room acoustic measurement example is presented. The goal was to lower the background noise in the 100-300 Hz band within the same measurement time. The measurements were made in a reverberation room using the same equipment and physical location (inputs and outputs of the system).

The speaker that was used to excite the test signals was a Genelec 8050A and the receiver was an omni-directional microphone attached to a Rion NL-32 sound level meter. The analog signal is transferred to 32-bit float wave files directly

by using an RME Fireface 800 external sound card module at a 48-kHz sampling rate.

Additional independent band noise in the 100-300 Hz was excited in the room during the measurements in steady state. The noise level in the room was 87 dB SPL, and when a sine sweep signal was excited it was 96 dB SPL.

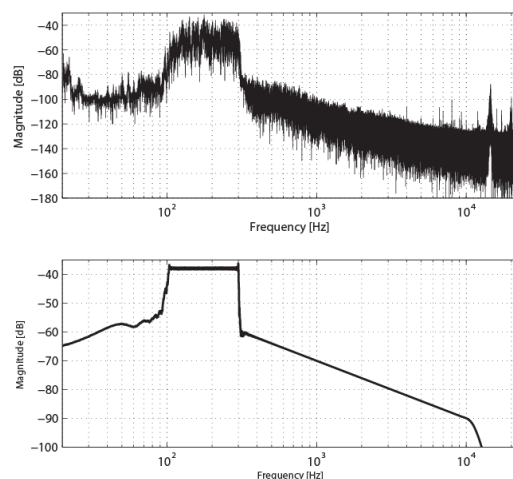


Figure 8. Top: observable background noise spectrum in the present measurement example; the 100-300 Hz noise was artificially excited using an independent loudspeaker.

Bottom: overall spectrum of a 3-segment monomial sweep focusing to the 100-300 band. The first segment [20..100 Hz] is a log-shape $[d, c, p] = [\omega_2 - 10, -1, 3]$, the second [100..300 Hz] is a linear $[d, c, p] = [\omega_2 + 10^7, 2, 3]$ and the third [300..24000 Hz] is a red sweep $[d, p] = [0, -1]$. Effect of time-windowing can be seen above 10 kHz.

The reference signal to which the comparison is made was the exponential sine sweep. The signals compared were a 3-segment monomial sine sweep (Fig. 8), a composite square sweep based on this signal, and a composite square sweep with an exponential mother sweep, all focusing to develop a better SNR in the 100..300 Hz range. Composite square sweeps contained two components where the wideband component was 15 dB attenuated. Signals were 30-second long.

Fig. 9 presents the obtained results. According to the expectations (Fig. 7), the noise levels using the optimized signals decreased and the forecasted improvement of about 10 dB was achievable in the targeted frequency range; and all signals delivered similar improvements there.

At higher frequencies the composite square sweep produced better results than the monomial sine sweeps which was due to the time-windowing of the sine sweep.

CONCLUSIONS

This paper presented a new family of sine sweeps capable of generating customizable sweep shapes. By customizing the sweep shapes the overall frequency response can be customized while the signal amplitude does not change. Such customization is now possible in the time-domain by using the proposed methods.

Sine, sparsely distorted and square sweep customizations were presented implemented by the following ways:

- Sweep rate customization (of the mother sine sweep) by means of analytic time-domain generation methods

- Crest factor increasing by means of frequency component customization using Lanczos-smoothed Fourier series
- Composite signal generation by mixing square signals sweeping in different bands simultaneously

By using such signals results with lower noise are obtainable. A room acoustic measurement example was presented to verify the applicability of the proposed method.

REFERENCES

- 1 H. Alrutz and M.R. Schroeder, "A fast Hadamard transform method for the evaluation of measurements using pseudorandom test signals," *Proc. of 11th International Congress on Acoustics*, Paris, 1983, pp. 235-238.
- 2 A.J. Berkhout, D. De Vries, and M.M. Boone, "A new method to acquire impulse responses in concert halls," *J. Acoust. Soc. Am.*, **68**, 1980, pp. 179-183.
- 3 Y. Suzuki, F. Asano, H. Kim, and T. Sone, "An optimum computer generated pulse signal suitable for the measurement of very long impulse responses," *J. Acoust. Soc. Am.* **97**, 1995, pp. 1119-1123.
- 4 S. Muller and P. Massarani, "Transfer-function measurement with sweeps," *J. Aud. Eng. Soc.*, **49**, 2001, pp. 443-471.
- 5 N. Moriya and Y. Kaneda, "Optimum signal for impulse response measurement that minimizes error caused by ambient noise," *J. Acoust. Soc. Japan*, **64**, 2008, pp. 695-701.
- 6 A. Farina, "Advancements in impulse response measurements by sine sweeps," *122nd AES Convention*, Paper 7121, Vienna, 2007, pp. 5-8.
- 7 C. Lanczos, *Applied analysis* (Dover Publications, 1988), pp. 225-229.
- 8 R. Hamming, *Numerical methods for scientists and engineers 2nd Ed.*, (Dover Publications, 1986), pp. 534-356.

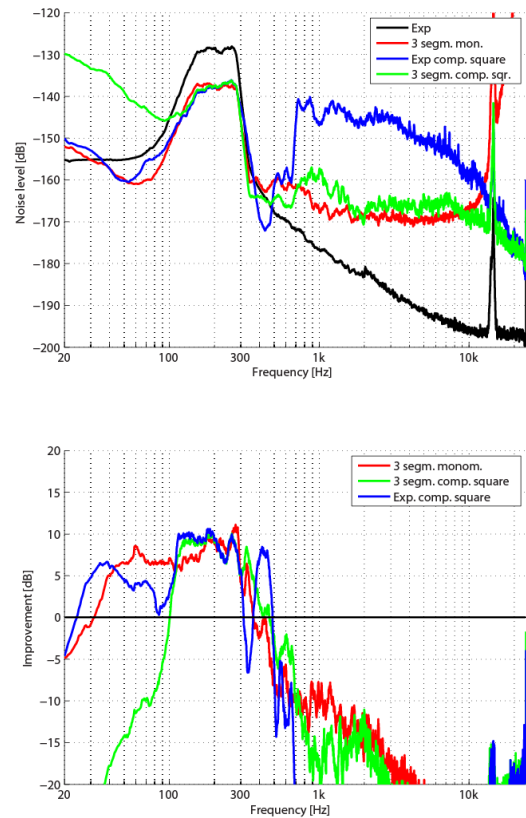


Figure 9. Background noise level in the impulse responses (top) and improvement compared to the exponential sine sweep (bottom) when using different excitation signals of the proposed method in the presence of excessive band-limited background noise in the 100-300 Hz band.